ACS APPLIED MATERIALS & INTERFACES

Research Article

www.acsami.org

Simple Ethanol Impregnation Treatment Can Enhance Photocatalytic Activity of TiO_2 Nanoparticles under Visible-Light Irradiation

Lina Kong,[†] Zhiqiang Jiang,[‡] Changhua Wang,[†] Fangxu Wan,[†] Yingying Li,[†] Liangzhuan Wu,[§] Jin-Fang Zhi,[§] Xintong Zhang,*[,†] Shijian Chen,*[,‡] and Yichun Liu[†]

[†]Center for Advanced Optoelectronic Functional Materials Research, and Key Laboratory for UV-Emitting Materials and Technology of Ministry of Education, Northeast Normal University, 5268 Renmin Street, Changchun 130024, China

[‡]School of Physics, Chongqing University, Shapingba, Chongqing 401331, China

[§]Key Laboratory of Photochemical Conversion and Optoelectronic Materials, Technical Institute of Physics and Chemistry, 29 Zhongguancun East Road, Haidian District, Beijing 100190, China

Supporting Information

ABSTRACT: Doping with impurities as well as introducing oxygen vacancies has been recognized as an important means to enhance photocatalytic activity of TiO_2 under visible-light irradiation. Here we report that simple ethanol impregnation followed with mild heat treatment (150−400 °C) can color TiO_2 nanoparticles and enhance visible-light photocatalytic activity of the material. The coloration and photocatalytic activity for β-naphthol and rhodamine B (RhB) degradation were observed to be dependent on heat-treatment temperature, and the highest activity as well as the most coloration was obtained at temperatures around 200 to 250 °C. Comprehensive analyses based on X-ray photoelectron spectroscopy (XPS) and electron paramagnetic resonance (EPR) investigations as well as first-principle density functional calculation suggest that the simple ethanol impregnation treatment leads to the generation of oxygen vacancy on TiO_2 surface which should be responsible for the coloration and enhanced photocatalytic activity.

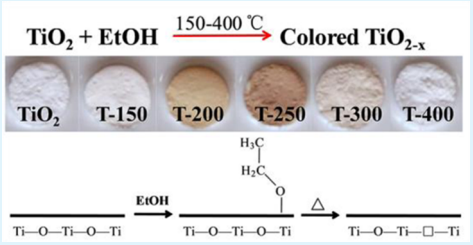

KEYWORDS: *TiO_2, visible-light photocatalyst, ethanol impregnation, oxygen vacancy, density functional calculation*

INTRODUCTION

Colored TiO_2 with considerable activity under visible light has received enormous attention due to its broad application in solar energy conversion and environmental cleanup.[1−4] In particular, doping has been regarded as an important way to enhance photocatalytic activity of TiO_2 under visible light.[5−7] Bulk doping, either with foreign elements[8,9] or via self-doping[10−12] (Ti^{3+} and oxygen vacancies), could render TiO_2 colored and exhibit photocatalytic activity under visible light. However, these defects often work as recombination centers during the migration of photogenerated charge carriers from the bulk to the surface. In this regard, doping only on the surface might be practically useful for extending the photoresponse of TiO_2 to visible light, since charge carriers trapped at surface doping levels are accessible to target substances near the surface, while undesired bulk recombination could be avoided. Several works have focused on surface doping. For instance, Cho et al. employed a rapid heating process to codope TiO_2 nanowires with tungsten and carbon on surface, which led to a significant enhancement in photoelectrochemical water splitting;[13] Chang et al. verified that surface doping is more beneficial than bulk doping to the photocatalytic activity of vanadium-doped TiO_2;[15] Kong et al. reported that decreasing the relative concentration ratio of bulk defects to surface defects in TiO_2 nanocrystals could significantly improve the separation efficiency of photogenerated electrons and holes, thus significantly enhancing photocatalytic efficiency.[14]

Apart from foreign doping, self-doping has only recently been recognized as an effective way to enhance photoactivity of TiO_2 in visible light.[16−18] The self-doping of TiO_2 often involves the generation of Ti^{3+} and oxygen vacancies (types of intrinsic defects) whose energy levels are below conduction band minimum and therefore can result in coloration of TiO_2 without the introduction of foreign elements.[19] Various methods, such as hydrogenation methods,[16] vacuum treatment,[10] plasma treatment,[20] chemical reduction,[21] as well as ion bombardment[22] have been adopted to self-dope TiO_2. However, these methods often result in both bulk and surface self-doping. Therefore, it is still interesting to develop a reliable method to do self-doping only on the surface.

It is well-known that lattice oxygen atoms on the surface of TiO_2 nanoparticles are likely to participate in reactions with adsorbed substances.[23−25] This motivated us to propose a novel approach to achieve self-doping of TiO_2 nanoparticles via thermal-activated decomposition of adsorbed organic molecules. It is expected that the doping could preferentially proceed on surface or subsurface layer via selecting volatile

Received: January 31, 2015
Accepted: March 23, 2015
Published: March 23, 2015

DOI: 10.1021/acsami.5b00888
ACS Appl. Mater. Interfaces 2015, 7, 7752−7758

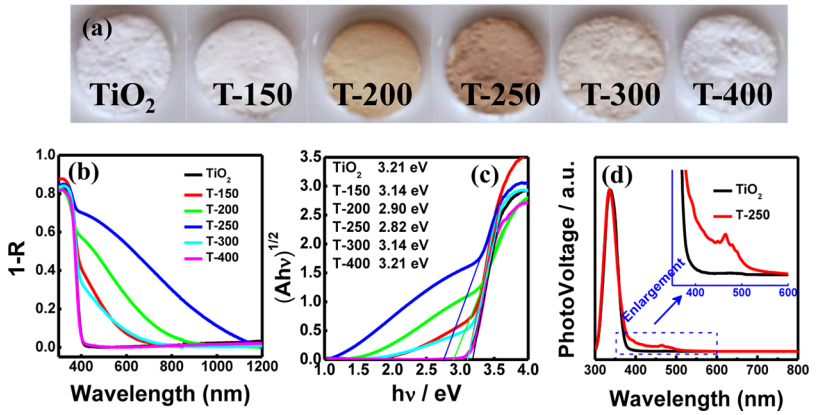

Figure 1. (a) Photograph of pristine TiO_2 and ethanol impregnated samples heating under different temperature. T-150, 150 °C; T-200, 200 °C; T-250, 250 °C; T-300, 300 °C; T-400, 400 °C. Note that the yellow color first increased then decreased with temperature. (b, c) UV−vis diffuses reflectance spectra and Tauc plot for the pristine TiO_2 and T-*n*. (d) SPS of the pristine TiO_2 and T-250 (inset is the magnified SPS patterns).

organic solvents as adsorbents. We report here that TiO_2 nanoparticles (commercial ST-01) were indeed colored after ethanol impregnation and mild heat treatment and exhibited enhanced photocatalytic activity for *β*-naphthol and rhodamine B degradation. The method could also be applied to the self-doping of other nanosized wide-band gap semiconductors, and various organic solvents other than ethanol should work well for the process.

EXPERIMENT

Material Synthesis. Anatase TiO_2 nanoparticles (ST-01) were from Ishihara Sangyo. Ethanol was from Beijing Chemical Reagent Company and used as received without any further purification. TiO_2 powders (1 g) were dispersed in ethanol (10 mL) under vigorous stirring for 1 h, and then, the powders were recovered by dried in air at 60 °C. Next, the ethanol-impregnated powders were transferred into a porcelain boat and heated at a temperature range from 150 to 400 °C for 1 h at a heating rate of 10 °C min^{-1} under ambient atmosphere. The pristine TiO_2 and ethanol impregnated followed with heat treated at 150 to 400 °C are denoted as TiO_2 and T-*n*, respectively (*n* = 150−400 for different heat treated temperature), hereafter for convenience. A series of different colored TiO_2 turned from white to light yellow and earthy yellow were obtained by varying the time and temperature of the heat treatment.

TiO_2 from different sources, e.g., Degussa P25, anatase TiO_2 (Beijing Chemical Reagent Company), as well as homemade TiO_2 microspheres[26] were also treated by the same way in order to evaluate the versatility of the method. Alternatively, different organic solvents such as acetic acid, isopropyl alcohol, acetone, acetyl acetone, acetaldehyde, and methanol were also tested instead of ethanol.

Material Characterization. UV−vis diffuse reflectance (DR) spectra of the samples were collected on a PerkinElmer UV WinLab spectrophotometer, and $BaSO_4$ was used as a reference. Surface photovoltage spectrum (SPS) measurements were carried out on a lab-made instrument.[27] Transmission electron microscope (TEM) images were acquired using a JEOL JEM-2100 instrument working at an acceleration voltage of 200 kV. Crystal structure and phase identification of the samples were performed by X-ray diffraction (XRD) (Rigaku, D/max-2500 X-ray diffractometer). X-ray photoelectron spectroscopy (XPS) experiments were performed on a VGESCALAB MKII instrument with a Mg K*α* ADES ($h\nu$ = 1253.6 eV) source. Electron paramagnetic resonance (EPR) measurements were conducted on an X-band CW-EPR Bruker ElEXSYS spectrometer in the X band (9.38 GHz) at 90 K equipped with a cylindrical cavity operating at 100 kHz field modulation.

Photocatalytic Experiments. Photocatalytic properties of the samples were investigated by measuring the photodegradation of *β*-naphthol and Rhodamine B (RhB) dye solution under ambient conditions. TiO_2 particles (0.1 g) were placed in 50 mL degradation solution: *β*-naphthol (150 mg/L solvent, acetonitrile:water = 1:99 v/v) and RhB (10 mg/L aqueous solution). A 150 W xenon lamp (Hayashi LA-410) was used as the simulated solar light source. Visible light was obtained with a 420 nm long-pass filter. Magnetic stirring of the suspension was continued throughout the reaction. Every 15 min, 3 mL aliquots of the solution were sampled and the absorption spectra of the reaction solutions were measured using a spectrometer (PerkinElmer UV WinLab spectrophotometer) to determine *β*-naphthol concentration from the absorption peak at 327 nm and the RhB concentration from the absorption peak at 552 nm.

DFT Calculations. The calculations were performed in the framework of the density functional theory (DFT), using the pseudopotential method with the projector augmented wave (PAW) potentials as implemented in the Vienna Ab-initio Simulation Package (VASP) code.[28] For the exchange-correlation energy, the generalized gradient approximation (GGA) with the form of the Perdew−Burke−Ernzerhof (PBE) was used.[29] The bulk anatase TiO_2 system was simulated using a periodic 2 × 2 × 1 supercell, which contained 16 Ti atoms and 32 O atoms, respectively. The energy cutoff of the wave function expanded in the plane-wave basis was set as 500 eV. For the Brillouinzone integration, 7 × 7 × 7 (for bulk system) and 5 × 5 × 1 (for surface system) Monkhorst-pack grids were used.

RESULTS AND DISCUSSION

TiO_2 powders (ST-01) usually stay their original white color after heating at 150 to 400 °C under ambient conditions. (Figure S1) However, after ethanol impregnation, the powders changed color when subjected to the same heat treatment. The color gradually changed from white to earthy yellow when increasing the heating temperature from 150 to 250 °C (Figure 1a). With further temperature increase, the color of TiO_2

DOI: 10.1021/acsami.5b00888
ACS Appl. Mater. Interfaces 2015, 7, 7752−7758

gradually faded to light yellow and white. Notably, the color (either light yellow or earthy yellow) of TiO_2 remained unchanged for several months at ambient conditions.

The colored TiO_2 samples exhibited broad absorption in the visible spectral region, and for the sample T-250, even extending to the near-infrared (NIR) region, as shown in UV−vis diffuse reflectance (DR) spectra (Figure 1b). The increased absorption in the visible region together with the red-shifted absorption onset was consistent with the color deepening of the samples. Similarly, the bandgap values, estimated from the sharply risen edge of the Tauc plot (Figure 1c), also changed with the treated temperature and were narrowed to 2.82 eV for the sample T-250. These spectral changes suggested that midgap states of broad energy distribution were introduced below the conduction band minimum by the ethanol impregnation treatment, which as a result extended the photoresponse range of TiO_2.

Surface photovoltage (SPV) measurements can give clear information about wavelength-dependent charge separation properties of semiconductor materials. As shown in Figure 1d, pristine TiO_2 exhibited a SPV threshold at 380 nm, consistent with its optical bandgap, but that of the sample T-250 was red-shifted to 510 nm; that is to say, visible light with wavelength shorter than 510 nm can induce effective charge separation. It should be noted that the absorption onset of the sample was actually down to 1100 nm, which implies carriers generated by long-wavelength excitation are prone to be confined at surface and thus to be silent in the SPV spectrum.

The colored TiO_2 powders remained anatase structures and their particle morphology also changed negligibly, as evidenced by XRD and TEM measurements. The grain size was estimated to 11.3, 11.0, 11.2, 11.0, 11.5, and 13.1 nm from the (101) peak of anatase for the pristine TiO_2 and T-150, T-200, T-250, T-300, and T-400, respectively. Besides the slight growth of T-400 (Figure 2a), there seems to be little change in the other samples. The TEM images in Figure 2b and c show that there was no change in either morphology or particle size for the pristine TiO_2 and T-250. The high-resolution TEM images in Figure 2d and e once again confirm that the anatase phase of TiO_2 remained unchanged after ethanol impregnation treatment by the coincident distance of (101) lattice spacing.

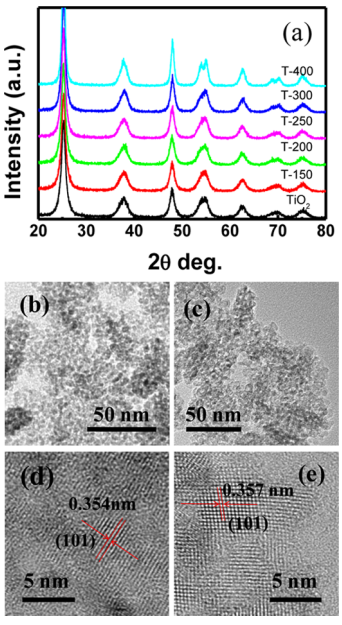

Figure 2. (a) XRD pattern of the pristine TiO_2 and T-*n*. (b−e) TEM and HRTEM images of the pristine TiO_2 and T-250 (b and d are for pristine TiO_2; c and e are for T-250).

XPS was employed to further investigate surface chemical bonding and estimate the ratio of different elements of the pristine and modified TiO_2 samples. Figure 3a shows the XPS spectra of Ti 2p and O 1s spectra of TiO_2 and the modified TiO_2 samples. Pristine TiO_2 showed Ti 2p states with a binding energy (BE) of 458.14 and 463.88 eV, consistent with the standard $2p_{3/2}$ and $2p_{1/2}$ binding energies for Ti^{4+} in anatase.[30] The peaks at 529.35 eV with a shoulder at 531.10 eV are attributed to O 1s peak of the TiO_2 samples, which are defined as O−Ti and O−H (surface hydroxyl band), respectively.[31] The atomic ratio of $O_{(O-Ti)}$/Ti of the pristine TiO_2 and the treated samples was calculated from the XPS spectra. The calculated results are presented in Figure 3b and Table 1. The atomic ratios of $O_{(O-Ti)}$/Ti for pristine TiO_2 and the modified samples obeyed the order of the pristine TiO_2 (1.98) > T-400 (1.92) > T-150 (1.85) ~ T-300 (1.83) > T-200 (1.78) ~ T-250 (1.78). Thus, surface oxygen vacancies are present in modified TiO_2 samples identified by the surface sensitive XPS measurement and the amount of surface oxygen vacancies defects vary with the heat treatment temperature which shows the same trend as the color change of the modified samples shown in Figure 1a, i.e., with the color deepening of the samples, the atomic ratios of $O_{(O-Ti)}$/Ti synchronously decrease, hence it

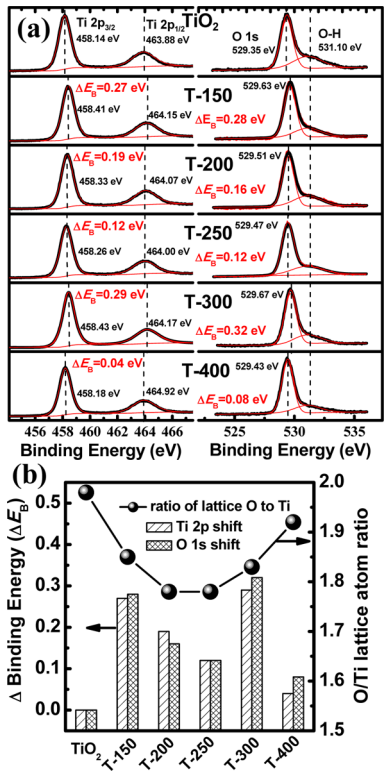

Figure 3. (a) XPS spectra of Ti 2p and O 1s spectra of TiO_2 and modified TiO_2 samples. (b) Movement of the Ti 2p and O 1s binding energy and variation of the atom ratio of lattice oxygen and lattice titanium for the TiO_2 and modified samples. (All the peak maxima were calibrated to C 1s at 284.6 eV, which was mainly ascribed to remnant organic precursors not completely removed from the employed TiO_2.).

DOI: 10.1021/acsami.5b00888
ACS Appl. Mater. Interfaces 2015, 7, 7752−7758

Table 1. XPS Results for Pristine TiO_2 and Modified Samples

sample	O−Ti (eV)	O−H (eV)	Ti $2p_{3/2}$ (eV)	Ti $2p_{1/2}$ (eV)	O/Ti[a] ratio
TiO_2	529.35	531.10	458.14	463.88	1.98
T-150	529.63		458.41	464.15	1.85
T-200	529.51		458.33	464.07	1.78
T-250	529.47		458.26	464.00	1.78
T-300	529.67		458.43	464.17	1.83
T-400	529.43		458.18	463.92	1.92

[a]The atom ratio of lattice oxygen and lattice titanium of TiO_2 and modified samples.

can be deduced that the coloration of TiO_2 should be related to the oxygen vacancy defects on TiO_2 surface. Simultaneously, compared with pristine TiO_2, all the colored samples exhibit a higher binding energy of both Ti 2p and O 1s (surface lattice oxygen) as listed in Figure 3b and Table 1. It is believed that the shift of binding energy of the Ti 2p and O 1s to a higher value could be attributed to the increased concentration of surface O vacancies. In fact, Xing et al.[10] also observed the synchronous shift of XPS peak of Ti 2p and O 1s to higher binding energy in TiO_2, and they ascribed it to the formation of neighboring oxygen vacancies showing a high electron-attracting effect.[32,33] However, the T-200 and T-250 samples did not show the highest variation of binding energy (ΔE_B) as expected, this could be the result of that a few Ti^{3+} defects were generated in the T-200 and T-250 samples for their highest oxygen vacancy concentration. The existence of Ti^{3+} in TiO_2 would lead the O 1s and Ti 2p shift to lower binding energy.[21,34]

Electron paramagnetic resonance (EPR) spectra were further employed to gain more detailed information on the nature of defects in colored TiO_2 samples. In the EPR spectra (Figure 4),

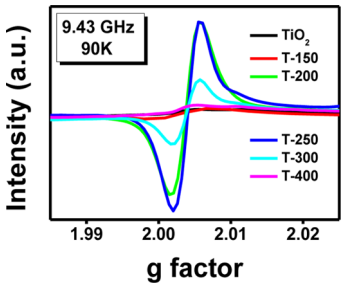

Figure 4. EPR spectra of pristine and modified samples.

it can be observed that the modified samples with the same measured weight exhibit isotropic resonances EPR signal at g = 2.003, which is the characteristic feature of $O_2^{\bullet-}$ radicals.[20,35] It is well-known that $O_2^{\bullet-}$ can be generated from the interaction of absorb atmospheric O_2 with the surface oxygen vacancy sites.[2,36] The generation of the $O_2^{\bullet-}$ is dependent on the nature and amount of the surface oxygen vacancy sites in the catalyst.[37,38] Once again, the intensity of the EPR signal kept pace with the visible-light absorption intensity in TiO_2 samples, following the order of T-250 > T-200 > T-300 > T-150 ~ T-400 ~ TiO_2. EPR signals in pristine TiO_2, T-150, and T-400 samples were nearly silent, suggesting a small amount of surface oxygen vacancies was contained in these samples.

Photocatalytic activity of the modified and pristine TiO_2 was assessed by monitoring the degradation of β-naphthol solution under visible light (420−700 nm) irradiation. β-naphthol is the starting material of azo dyes and is frequently used as a model water pollutant.[39] Since β-naphthol is adsorbed negligibly on the surface of TiO_2 samples (Figure S2a) and is insensitive to the visible light, any decrease in concentration of the chemicals during visible light irradiation should be related to photocatalytic processes on the TiO_2 samples. Figure 5a and b trace

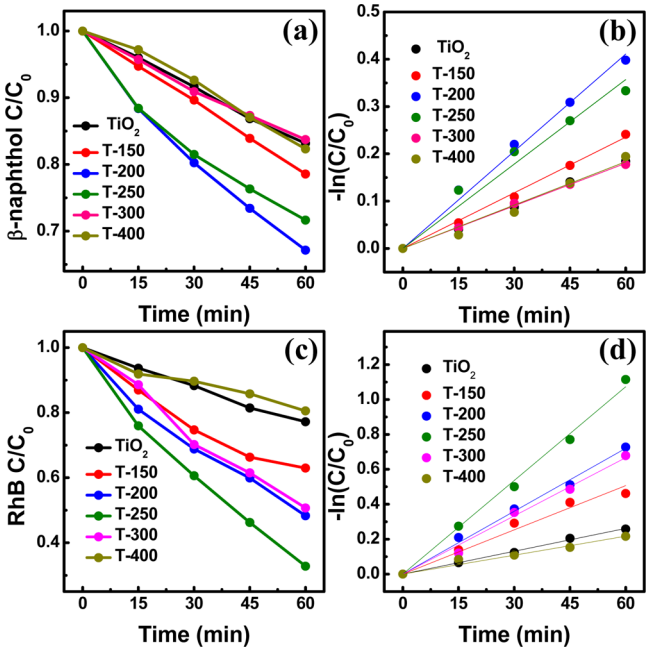

Figure 5. Degradation kinetics of (a, b) β-naphthol and (c, d) rhodamine B (RhB) dye over the pristine and modified TiO_2 samples under visible-light irradiation (420−700 nm).

the photodegradation of β-naphthol solution with TiO_2 samples. The photocatalytic degradation of β-naphthol follows the pseudo first-order kinetics, and apparent rate constants calculated from Figure 5b are listed in Table 2. The photodegradation of β-naphthol with pristine TiO_2 appears to be quite slow. But it is significantly accelerated with the modified TiO_2 samples, indicating that the ethanol impregnation and subsequent heat treatment indeed can enhance the photocatalytic activity of TiO_2 under visible light excitation. In particular, the colored TiO_2 samples, i.e.T-200, T-250, and T-300, perform better than other white TiO_2 samples, suggesting better absorption of visible light is responsible for the faster photocatalytic degradation of β-naphthol.

The photodegradation of rhodamine B (RhB) was also conducted with pristine and the modified TiO_2 samples under visible light irradiation in order to understand better the effect of ethanol impregnation treatment. Rhodamine B is a kind of dye that strongly absorbs visible light. Its photodegradation with TiO_2 proceeds in two manners, one is photocatalytic decomposition by TiO_2, while the other is sensitized photodegradation related to the excitation of the surface-adsorbed RhB molecules. Dark adsorption experiments show that the ethanol impregnation treatments increase the adsorption rate of RhB on TiO_2 samples, by a sequence of T-300 > T-400 > T-250 ~ T-200 > TiO_2 > T150 (Figure S2b). But under visible light irradiation, RhB is photodegraded with TiO_2 samples by much faster rates than the dark adsorption (Figure 5c and d). Table 2 also lists the pseudo first-order rate constants for RhB

DOI: 10.1021/acsami.5b00888
ACS Appl. Mater. Interfaces 2015, 7, 7752−7758

Table 2. Apparent Rate Constants (k) of β-Naphthol and RhB Dye Degradation under Visible Light (420−700 nm) with TiO_2 Samples

sample	TiO_2	T-150	T-200	T-250	T-300	T-400
$k_{\beta\text{-naphthol}}$ (min^{-1})	0.00306	0.00392	0.00685	0.00595	0.00300	0.00305
k_{RhB} (min^{-1})[a]	0.00404	0.00827	0.01160	0.01754	0.00969	0.00309

[a]The rate constants are calculated by subtracting the dark adsorption from photodegradation data.

photodegradation with the TiO_2 samples after removal of the contribution of dark adsorption. Again, the ethanol impregnation treatment enhances the photodegradation of RhB on TiO_2, and the three colored TiO_2 samples, i.e. T-200, T-250, and T-300, exhibit faster degradation rates for RhB dye than other white samples. It is interesting to note that the T-250 sample exhibits 1.8 times higher k_{RhB} than the T-300 and 5.7 times higher than the T-400, despite of its poorer adsorption ability for RhB, suggesting photocatalyzed decomposition of RhB is the dominant process on these colored TiO_2 samples. Therefore, the ethanol impregnation approach employed here successfully produces colored TiO_{2-x} catalysts with enhanced photocatalytic activity under visible light irradiation.

We simulated the ethanol impregnation treatment by heating TiO_2 powders in ethanol atmosphere in a closed vessel. Briefly, 50 mg TiO_2 powders were uniformly spread in a 500 mL Pyrex glass vessel filled with synthetic air. The powders were heated to 200 °C and then 4.15 μmol of ethanol was injected into the vessel to reach a concentration of 200 ppmv. The composition of gas phase was monitored with a gas chromatograph. Soon after the injection, acetaldehyde was detected in the gas phase. The concentration of acetaldehyde gradually increased in the first 30 min (Figure S3). Meanwhile, the color of TiO_2 powders gradually turned to yellow from white. When extending the reaction time to 90 min, no acetaldehyde could be detected in the gas phase, while the concentration of CO_2 increased markedly. These experimental observations manifest that the heated TiO_2 powders can oxidize ethanol, even complete mineralize ethanol to CO_2, at the cost of loss of lattice oxygen atoms. Possible reactions involved in the process can be expressed aswhere O_O and V_O represent lattice oxygen and oxygen vacancy, respectively.

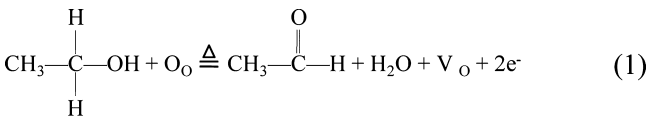

$$CH_3CH(OH) + O_O \triangleq CH_3C(=O)H + H_2O + V_O + 2e^- \quad (1)$$

We further performed first-principle density functional theory (DFT) calculations to make sense of the formation of oxygen vacancies by the simple ethanol impregnation treatment. Formation energies were calculated to describe the differences between the approach of ethanol impregnation followed by thermal treatment and the simple thermal annealing approach. The simple thermal annealing approach can be described as removing an oxygen atom from TiO_2 crystal to a reservoir of energy μ_0, referenced to the energy of oxygen in an isolated O_2 molecular. Therefore, the formation energy of this approach would be defined as $E_{f1} = (E_{VO} + \mu_0) - E_{TiO2}$, where E_{TiO2} is the energy of 2 × 2 × 1 TiO_2 supercell, which contains 16 Ti atoms and 32 O atoms; E_{VO} is the energy of the same 2 × 2 × 1 TiO_2 supercell with one oxygen vacancy; and μ_0 is the chemical potential of removal oxygen atom from TiO_2 lattice. The other approach (used in this work) would be divided into two processes: first, ethanol molecules are adsorbed at Ti^{4+} sites on the anatase TiO_2 (101) surface to form ethoxides and, second, the ethoxides molecules would undergo β elimination on heating to form acetaldehyde, leaving oxygen vacancies on the TiO_2 surface. Hence, the formation energy of this approach would be expressed as $E_{f2} = \Delta E_{P1} + \Delta E_{P2}$, where ΔE_{P1} and ΔE_{P2} are the energy differences of the two processes. $\Delta E_{P1} = E_{TiO2-C2H6O} - (E_{TiO2} + E_{C2H6O})$, where $E_{TiO2-C2H6O}$ is the total energy of ethanol adsorbed on the TiO_2 (101) surface and E_{C2H6O} is the energy of an ethanol molecule; $\Delta E_{P2} = (E_{VO} + E_{H2O} + E_{C2H4O}) - E_{TiO2-C2H6O}$, where E_{H2O} and E_{C2H4O} are the energy of a water and acetaldehyde molecules, respectively. With these definitions, the formation energy denotes how difficult the reaction is, and lower formation energy is more favorable to create oxygen vacancy with lower formation energy.

After full relaxation, the formation energies are calculated to be 0.41 eV for the simple thermal annealing approach, and −1.67 eV for the approach of ethanol impregnation followed by thermal treatment, respectively. It is clear that it is much easier to create oxygen vacancies at the TiO_2 surface by the ethanol impregnation approach with the lower formation energy of −1.67 eV.

We also conducted several comparative experiments to illustrate the universality of the process in coloration of TiO_2. In one experiment, several kinds of TiO_2 photocatalysts, including Degussa P25 homemade TiO_2 microspheres, and micrometer-sized anatase TiO_2 were used instead of ST-01. All three samples showed color change after ethanol impregnation and heat treatment (Figure S4a), suggesting the as-adopted surface doping method is generally suitable for various TiO_2. Besides the replacement of TiO_2, other solvents such as acetic acid, isopropanol, acetone, acetylacetone, acetaldehyde, and methanol are also used instead of ethanol. Similarly, all of these solvents colored TiO_2 as shown in Figure S4b. The activities of these samples were also evaluated by photocatalytic degradation of β-naphthol under visible-light irradiation. Several typical data is shown in Figure 6. Once again, the colored TiO_2 exhibited higher photocatalytic activity than that of untreated TiO_2 under visible-light irradiation.

CONCLUSION

In summary, we developed a simple method for the synthesis of colored TiO_2 through ethanol impregnation followed with mild heat treatment. Such colored TiO_2 possesses an enhanced visible-light absorption capability and superior photocatalytic activities for degradation of β-naphthol and rhodamine B under visible-light irradiation. XPS and EPR measurement results proved the existence of oxygen vacancies on TiO_2 surface that contribute to extending the visible-light absorption. The first-principle density functional (DFT) calculation indicated that it is much easier to create oxygen vacancy defects at the surface of TiO_2 by the approach of ethanol impregnation with the lower formation energy. Lastly, the method adopted here is not limited to TiO_2 and can be applied to the self-doping of other

DOI: 10.1021/acsami.5b00888
ACS Appl. Mater. Interfaces 2015, 7, 7752−7758

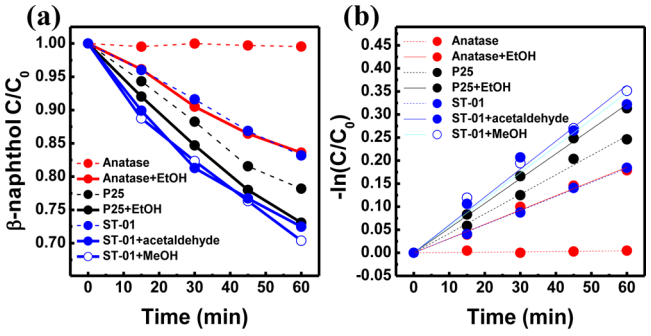

Figure 6. Degradation kinetics of β-naphthol over several TiO_2 samples under visible light irradiation: (red circles) anatase TiO_2 without and with ethanol impregnation; (black circles) Degussa P25 without and with ethanol impregnation; (blue circles) ST-01 without and with acetaldehyde or methanol impregnation. The samples are all heated at 250 °C for 1 h after impregnation.

nanosized wide-bandgap semiconductors for visible-light photocatalysis.

■ ASSOCIATED CONTENT

Supporting Information

Photographs of heat-treated TiO_2 samples without and with solvent impregnation, dark adsorption data of β-naphthol and RhB over the pristine TiO_2 and modified samples, time course of acetaldehyde generation during ethanol decomposition over heated TiO_2 samples. This material is available free of charge via the Internet at http://pubs.acs.org.

■ AUTHOR INFORMATION

Corresponding Authors

*E-mail: xtzhang@nenu.edu.cn. Fax: +86 431 85099772. Tel.: +86 431 85099772 (X.Z.).
*E-mail: sjchen@cqu.edu.cn. Tel.: +86 23 65678362 (S.C.).

Notes

The authors declare no competing financial interest.

■ ACKNOWLEDGMENTS

This work was supported by the Natural Science Foundation of China (Grant Nos. 51072032, 91233204, 11304406, 51372036, and 51102001), the Key Project of Chinese Ministry of Education (No 113020A), the Specialized Research Fund for the Doctoral Program of Higher Education (20120043110002), the National Basic Research Program (2012CB933703), the Fundamental Research Funds for the Central Universities (12SSXM001), the 111 project (No. B13013), and the International Science & Technology Cooperation Program of China (2013DFG50150)

■ REFERENCES

(1) Asahi, R.; Morikawa, T.; Ohwaki, T.; Aoki, K.; Taga, Y. Visible-Light Photocatalysis in Nitrogen-Doped Titanium Oxides. *Science* **2001**, *293*, 269−271.
(2) Di Valentin, C.; Finazzi, E.; Pacchioni, G.; Selloni, A.; Livraghi, S.; Paganini, M. C.; Giamello, E. N-Doped TiO_2: Theory and Experiment. *Chem. Phys.* **2007**, *339*, 44−56.
(3) Di Valentin, C.; Pacchioni, G.; Selloni, A. Reduced and n-Type Doped TiO_2: Nature of Ti^{3+} Species. *J. Phys. Chem. C* **2009**, *113*, 20543−20552.
(4) Fu, R.; Gao, S.; Xu, H.; Wang, Q.; Wang, Z.; Huang, B.; Dai, Y. Fabrication of Ti^{3+} Self-doped TiO2(A) Nanoparticle/TiO_2(R) Nanorod Heterojunctions with Enhanced Visible-Light-Driven Photocatalytic Properties. *RSC Adv.* **2014**, *4*, 37061−37069.
(5) Fujishima, A.; Zhang, X.; Tryk, D. A. TiO_2 Photocatalysis and Related Surface Phenomena. *Surf. Sci. Rep.* **2008**, *63*, 515−582.
(6) Hong, X.; Wang, Z.; Cai, W.; Lu, F.; Zhang, J.; Yang, Y.; Liu, Y. Visible-Light-Activated Nanoparticle Photocatalyst of Iodine-Doped Titanium Dioxide. *Chem. Mater.* **2005**, *17*, 1548−1552.
(7) Irie, H.; Watanabe, Y.; Hashimoto, K. Nitrogen-Concentration Dependence on Photocatalytic Activity of $TiO_{2-x}N_x$ Powders. *J. Phys. Chem. B* **2003**, *107*, 5483−5486.
(8) Liao, W.; Yang, J.; Zhou, H.; Murugananthan, M.; Zhang, Y. Electrochemically Self-Doped TiO_2 Nanotube Arrays for Efficient Visible Light Photoelectrocatalytic Degradation of Contaminants. *Electrochim. Acta* **2014**, *136*, 310−317.
(9) Sakthivel, S.; Kisch, H. Daylight Photocatalysis by Carbon-Modified Titanium Dioxide. *Angew. Chem., Int. Ed.* **2003**, *42*, 4908−4911.
(10) Xing, M.; Zhang, J.; Chen, F.; Tian, B. An Economic Method to Prepare Vacuum Activated Photocatalysts with High Photo-Activities and Photosensitivities. *Chem. Commun.* **2011**, *47*, 4947−4949.
(11) Yu, J.; Xiang, Q.; Zhou, M. Preparation, Characterization and Visible-Light-Driven Photocatalytic Activity of Fe-doped Titania Nanorods and First-Principles Study for Electronic Structures. *Appl. Catal. B* **2009**, *90*, 595−602.
(12) Zou, Z.; Ye, J.; Sayama, K.; Arakawa, H. Direct Splitting of Water Under Visible Light Irradiation with an Oxide Semiconductor Photocatalyst. *Nature* **2001**, *414*, 625−627.
(13) Cho, I. S.; Lee, C. H.; Feng, Y.; Logar, M.; Rao, P. M.; Cai, L.; Zheng, X. Codoping Titanium Dioxide Nanowires with Tungsten and Carbon for Enhanced Photoelectrochemical Performance. *Nat. Commun.* **2013**, *4*, 1723.
(14) Kong, M.; Li, Y.; Chen, X.; Tian, T.; Fang, P.; Zheng, F.; Zhao, X. Tuning the Relative Concentration Ratio of Bulk Defects to Surface Defects in TiO_2 Nanocrystals Leads to High Photocatalytic Efficiency. *J. Am. Chem. Soc.* **2011**, *133*, 16414−16417.
(15) Chang, S.-m.; Liu, W.-s. Surface Doping is More Beneficial than Bulk Doping to the Photocatalytic Activity of Vanadium-Doped TiO_2. *Appl. Catal. B* **2011**, *101*, 333−342.
(16) Chen, X.; Liu, L.; Yu, P. Y.; Mao, S. S. Increasing Solar Absorption for Photocatalysis with Black Hydrogenated Titanium Dioxide Nanocrystals. *Science* **2011**, *331* (6018), 746−750.
(17) Sakthivel, S.; Janczarek, M.; Kisch, H. Visible Light Activity and Photoelectrochemical Properties of Nitrogen-Doped TiO_2. *J. Phys. Chem. B* **2004**, *108*, 19384−19387.
(18) Dong, J.; Han, J.; Liu, Y.; Nakajima, A.; Matsushita, S.; Wei, S.; Gao, W. Defective Black TiO_2 Synthesized via Anodization for Visible-Light Photocatalysis. *ACS Appl. Mater. Interfaces* **2014**, *6*, 1385−1388.
(19) Naldoni, A.; Allieta, M.; Santangelo, S.; Marelli, M.; Fabbri, F.; Cappelli, S.; Dal Santo, V. Effect of Nature and Location of Defects on Bandgap Narrowing in Black TiO_2 Nanoparticles. *J. Am. Chem. Soc.* **2012**, *134*, 7600−7603.
(20) Nakamura, I.; Negishi, N.; Kutsuna, S.; Ihara, T.; Sugihara, S.; Takeuchi, K. Role of Oxygen Vacancy in the Plasma-Treated TiO_2 Photocatalyst with Visible Light Activity for NO Removal. *J. Mol. Catal. A: Chem.* **2000**, *161*, 205−212.
(21) Tan, H.; Zhao, Z.; Niu, M.; Mao, C.; Cao, D.; Cheng, D.; Feng, P.; Sun, Z. A Facile and Versatile Method for Preparation of Colored TiO_2 with Enhanced Solar-Driven Photocatalytic Activity. *Nanoscale* **2014**, *6*, 10216−10223.
(22) Feibelman, P. J.; Knotek, M. L. Reinterpretation of Electron-Stimulated Desorption Data from Chemisorption Systems. *Phys. Rev. B* **1978**, *18*, 6531−6539.
(23) Li, Y.; Huang, J.; Peng, T.; Xu, J.; Zhao, X. Photothermocatalytic Synergetic Effect Leads to High Efficient Detoxification of Benzene on TiO_2 and Pt/TiO_2 Nanocomposite. *ChemCatChem.* **2010**, *2*, 1082−1087.
(24) Panayotov, D. A.; Morris, J. R. Thermal decomposition of a chemical warfare agent simulant (DMMP) on TiO_2: adsorbate

DOI: 10.1021/acsami.5b00888
ACS Appl. Mater. Interfaces 2015, 7, 7752−7758

reactions with lattice oxygen as studied by infrared spectroscopy. *J. Phys. Chem. C* **2009**, *113*, 15684−15691.
(25) Wachs, I. E.; Jehng, J. M.; Ueda, W. J. Determination of The Chemical Nature of Active Surface Sites Present on Bulk Mixed Metal Oxide Catalysts. *Phys. Chem. B* **2005**, *109*, 2275−2284.
(26) Yang, J. K.; Zhang, X. T.; Wang, C. H.; Sun, P. P.; Wang, L. L.; Xia, B.; Liu, Y. C. Solar Photocatalytic Activities of Porous Nb-Doped TiO_2 Microspheres Prepared by Ultrasonic Spray Pyrolysis. *Solid State Sci.* **2012**, *14*, 139−144.
(27) He, D.; Wang, L.; Xu, D.; Zhai, J.; Wang, D.; Xie, T. Investigation of Photocatalytic Activities over $Bi_2WO_6/ZnWO_4$ Composite under UV Light and its Photoinduced Charge Transfer Properties. *ACS Appl. Mater. Interfaces* **2011**, *3*, 3167−3171.
(28) Kresse, G.; Hafner, J. Ab Initio Molecular Dynamics for Liquid Metals. *Phys. Rev. B* **1993**, *47*, 558−561.
(29) Perdew, J. P.; Wang, Y. Accnrate and Simple Analytic Representation of the Electron-Gas Correlation Energy. *Phys. Rev. B* **1992**, *45*, 13244−13249.
(30) Sen, S. K.; Riga, J.; Verbist, J. 2s and 2p X-ray Photoelectron Spectra of Ti^{4+} Ion in TiO_2. *Chem. Phys. Lett.* **1976**, *39*, 560−564.
(31) Cappelletti, G.; Ardizzone, S.; Bianchi, C. L.; Gialanella, S.; Naldoni, A.; Pirola, C.; Ragaini, V. Photodegradation of Pollutants in Air: Enhanced Properties of Nano-TiO_2 Prepared by Ultrasound Nanoscale. *Res. Lett.* **2009**, *4*, 97−105.
(32) Kumar, P. M.; Badrinarayanan, S.; Sastry, M. Nanocrystalline TiO_2 Studied by Optical, FTIR and X-ray Photoelectron Spectroscopy: Correlation to Presence of Surface States. *Thin Solid Films* **2000**, *358*, 122−130.
(33) Conesa, J. C.; Soria, J. Reversible Ti^{3+} Formation by H_2 Adsorption on M/TiO_2 Catalysts. *J. Phys. Chem.* **1982**, *86*, 1392−1395.
(34) Fu, R.; Gao, S.; Xu, H.; Wang, Q.; Wang, Z.; Huang, B.; Dai, Y. Fabrication of Ti^{3+} Self-Doped TiO_2 (A) Nanoparticle/TiO_2(R) Nanorod Heterojunctions with Enhanced Visible-light-Driven Photocatalytic Properties. *RSC Adv.* **2014**, *4*, 37061−37069.
(35) Komaguchi, K.; Maruoka, T.; Nakano, H.; Imae, I.; Ooyama, Y.; Harima, Y. Electron-Transfer Reaction of Oxygen Species on TiO_2 Nanoparticles Induced by Sub-Band-Gap Illumination. *J. Phys. Chem. C* **2010**, *114*, 1240−1245.
(36) Hirakawa, T.; Yawata, K.; Nosaka, Y. Photocatalytic Reactivity for $O_2^{\cdot-}$ and $OH^{\cdot}$ Radical Formation in Anatase and Rutile TiO_2 Suspension as the Effect of H_2O_2 Addition. *Appl. Catal., A* **2007**, *325*, 105−111.
(37) Coronado, J. M.; Soria, J. ESR Study of the Initial Stages of the Photocatalytic Oxidation of Toluene over TiO_2 Powders. *Catal. Today* **2007**, *123*, 37−41.
(38) Carter, E.; Carley, A. F.; Murphy, D. M. Evidence for O_2-Radical Stabilization at Surface Oxygen Vacancies on Polycrystalline TiO_2. *J. Phys. Chem. C* **2007**, *111*, 10630−10638.
(39) Mishra, V. S.; Mahajuni, V. V.; Joshi, J. B. Wet Air Oxidation. *Ind. Eng. Chem. Res.* **1995**, *34*, 2.

DOI: 10.1021/acsami.5b00888
ACS Appl. Mater. Interfaces 2015, 7, 7752−7758